

MET O 19 BRANCH MEMORANDUM NO 83

High Resolution Polar Stereographic
Sea Surface Temperature Images from
AVHRR data.

by

R.W.Pescod, R.W.Saunders and J.R.Eyre

May 1986

Met. Office Unit (Met.O.19c)
Hooke Institute for Atmospheric Research
Clarendon Laboratory
Oxford OX1 3PU

NOTE:

This paper has not been published. Permission to quote from it should be obtained from the Assistant Director (Satellite Meteorology), Meteorological Office, London Road, Bracknell, Berks RG12 2SZ.

High Resolution Polar Stereographic Sea Surface Temperature Images from AVHRR data.

1. INTRODUCTION

Sea surface temperature (SST) data around the British Isles are currently available to forecasters in the form of a 5 day mean contour chart updated three times a week. These charts are produced from ship and buoy reports averaged over a five day period. Data from the Advanced Very High Resolution Radiometer (AVHRR) on board the TIROS-N/NOAA series of polar orbiting satellites (Schwalb 1978) can potentially give a 5 day mean SST chart with a greatly improved spatial resolution.

The Meteorological Office plans to introduce a new computer system, AUTOSAT 2, to be used for processing digital satellite data. The availability of real-time High Resolution Picture Transmission data (HRPT) from the NOAA satellites makes possible the generation of new operational products from the AVHRR data. This paper describes an experimental scheme to produce a new SST product from the AVHRR data around the British Isles. It is intended to demonstrate how this or similar products could be derived operationally by AUTOSAT 2.

2. PROCESSING SCHEME

2.1 COMPUTATION OF SEA SURFACE TEMPERATURE

A general outline of the processing scheme is shown in figure 1 and described below. The details of the programs used on the Meteorological Office computers, HOMER and HERMES, to process the data are described in appendix A.

The raw input data are those received from the spacecraft as part of the HRPT data. They consist of upwelling radiance measurements made at five wavelengths (channels 1-5 centred at $0.53\mu\text{m}$, $0.85\mu\text{m}$, $3.7\mu\text{m}$, $10.7\mu\text{m}$ and $11.8\mu\text{m}$ respectively) over a field of view of about 1 km at the sub-satellite point. Each radiance is in the form of a 10 bit count (i.e. a value between 0 and 1023). The raw data stream is unpacked from 10 to 16 bits for the channels required (1, 2, 4, 5 for the day pass and 3, 4, 5 for the night pass). The visible and near infra-red counts (channels 1 and 2) are converted to radiances and then to reflectances by dividing by the incident solar radiation within the filter response function of each channel. The infra-red radiances (channels 3, 4 and 5) are converted to brightness temperature using the scheme outlined by Lauritson et al. (1979) including the non-linearity correction given by NOAA for channels 4 and 5.

An earth location file is also computed for the image. Because of the large amount of data in an AVHRR image, it is not practicable to compute the latitude/longitude of every pixel in the image. As a compromise the locations of every 32nd pixel across and along the pass are computed and retained in a file. These locations are computed by first predicting the position of the spacecraft above the earth at a known time from a recent set of orbital elements (received from NOAA over the global telecommunication system) and then applying the satellite scan geometry to determine the locations of pixels along a scan line. The predicted position of the spacecraft above the earth is usually in error by less than ten kilometres but occasionally errors in the along-track direction can be more than this. To correct for this error a coastline can be computed from the location file which is then displayed over the image. Any offsets between the computed coastline and the actual coastline are then immediately obvious, and by interactively matching the two coastlines these offsets can be determined. The location file is then recomputed including these offsets. Obviously this correction procedure is only possible when there is at least some cloudfree coast within the image. The corrected location file is used by most of the subsequent processing steps.

The reflectances and brightness temperatures are used in a cloud detection scheme, which identifies cloudfree pixels, from which surface quantities can be derived. The scheme to detect cloudfree pixels is described in detail by Saunders (1986). Each pixel must pass five independent checks for cloud contamination, different tests are applied according to whether it is day or night. The first test is a gross infra-red temperature threshold which rejects pixels which are much colder than the climatological SST minus the expected atmospheric correction. As many as 50% of all pixels in the image are rejected by this test. The second test is a spatial uniformity check which relies on the fact that the brightness temperatures of cloudfree pixels will only vary slowly within a small array whereas cloud contaminated pixels will have a large variation in brightness temperature. During the day (i.e. solar elevation greater than 10 degrees) a visible reflectance check is applied which rejects all pixels greater than a pre-defined reflectance as cloud contaminated. The fourth test examines the value of the ratio of the near infra-red reflectance (channel 2) to the visible reflectance (channel 1). Cloudy pixels have a ratio close to unity whereas cloudfree ocean is around 0.5 and cloudfree land greater than 1.5. The final test uses the difference in brightness temperatures between the 11 and 12 μm infra-red channels. Large differences imply the pixel is partially filled with thick cloud or completely filled with optically thin cloud. At night the third and fourth tests described above cannot be used as the visible reflectance data are not available. Instead use is made of the 3.7 μm channel (when the noise

level is acceptably low). The third test at night examines the difference in brightness temperatures between the 11 and 3.7 μm channels, this detects low cloud or fog (Eyre et al. 1984). The fourth test at night looks at the difference between the brightness temperatures in the 3.7 and 12 μm channels, which is similar to the fifth day-time test for detecting partially cloudy pixels or thin cirrus cloud. The pixels which pass all of these tests are then assumed to be cloudfree.

The cloudfree infra-red brightness temperatures are then converted to a sea surface temperature using the 'split window' relationship described by Llewellyn-Jones et al. (1984) to remove atmospheric effects. It takes the form of a linear combination of the 11 and 12 μm channels:

$$\text{SST} = C_0 + C_1 T_4 + C_2 T_5 \quad (1)$$

where SST is the sea surface temp in degrees K and T_4 and T_5 are the brightness temperatures in channels 4 and 5. The regression coefficients C_i vary with "airmass" (i.e. secant of the satellite zenith angle). Values of SST are only computed through airmasses less than 2 so that data at the edge of the scan lines (less than 100 pixels from the edge) are not used. Although this scheme was designed for use over the sea it has been used with some success over land though differences between land and sea such as surface emissivity and atmospheric profile structure will lead to larger uncertainties. Values for the surface temperature are only computed from cloudfree pixels.

2.2 IMAGE REPROJECTION

The next step re-maps the SST image of the earth as viewed by the AVHRR instrument on to a polar stereographic projection plane (at 60 degrees latitude). This projection was chosen to be compatible with the current operational charts. The details of this projection process are given in appendix B. The display device which has been used is a SIGMEX Advanced Raster Graphic system (ARGS), with a resolution of 1024 by 1024 elements. With this in mind the map area and scale of projection (in km/pixel) on the screen are chosen. In this experiment a final product was created for a rectangular area in polar stereographic projection bounded by the latitude/longitude points 47.0 North -12.0 West and 60.0 North 10.0 East, i.e. about 1400 km by 1400 km. To select from one image all the pixels which may fall in this area, it is necessary to consider a swath about 1600 pixels wide from the full AVHRR image.

Location of every 32nd line and pixel is achieved as described above. The locations of all other pixels are then fixed by two-dimensional linear interpolation. The reprojection process allows a number of input images from different parts of a pass to be reprojected on to the same

polar stereographic plane. With this simple reprojection scheme, it is sometimes found that more than one input pixel mapped to a pixel in the output image, in these cases the last pixel to be reprojected was the one that was retained. Conversely it is found that towards the edges of an AVHRR swath, pixels in the reprojected image remained unfilled. This problem is overcome by assigning a pixel in the input image to up to 9 pixels (as necessary) in the output image for pixel positions in the input image greater than 824 pixels from the sub-orbital track.

The next step merges this reprojected data from different passes on several days (seven in this case) into one composite SST image. The procedure chosen (from several possibilities) was to retain the maximum SST value encountered for each pixel in the output image during the seven days. This helped to remove spurious low temperatures due to any remaining undetected cloud contamination. This does have the disadvantage that if a strong diurnal thermocline is present, significant diurnal variations in SST can occur (e.g. as seen by Saunders et al. 1982). This will bias the composite image to the warmest values and not give a true mean. With the advent of improved cloud detection algorithms this limitation could be removed and a true mean SST value computed. A better method of detection and removal of spurious pixel values (for whatever reason) could also be devised if a background field were available.

2.3 IMAGE ENHANCEMENT

To reduce the noise in the final image, a sliding median filter can be applied (a 3 by 3 filter was used in this case). This causes some reduction in the resolution of the product but this is acceptable because of the low horizontal variability of SST. After combining seven days of data, it was found that the final image contained areas which had been cloud contaminated on all fourteen passes. This resulted in some data voids. Voids of a few pixels were effectively removed by the median filter.

3. DATA USED FOR THIS STUDY.

Operationally the data would be received and processed at Lasham and then transmitted to Bracknell over the METSATNET link (a new high speed telecommunications link between Lasham and Bracknell). The HRPT data used in this study however were obtained on computer compatible magnetic tapes from the University of Dundee. They consisted of one daytime and one nighttime NOAA 9 pass over the British Isles, for each day during the week 14-20 April 1985. This corresponds to overpass times of approximately 0300 and 1330 GMT. A list of the passes used is given in table 1. The data used in this experiment were not a carefully selected set of cloud-free data, but seven days of contiguous data during April 1985 during which typical cloud cover was

experienced.

4. RESULTS

The composite sea surface temperature image produced by the processing scheme described above is shown in figure 2. For comparison two conventional five day mean sea surface temperature charts used operationally for the same period are shown in figures 3a and 3b. These charts are produced using only observations from ships and buoys, and they represent the bulk water temperature to a depth of about one metre.

Comparing the conventional charts with the satellite product it can be seen that there is general agreement in absolute temperature values between them and the major features are discernible in both. One such feature is the tongue of warmer water off north west Scotland and Ireland. Another is the cold coastal strip of water flowing north up the Norwegian west coast as studied by Mork (1981). However there is far more detail in the satellite plot which cannot be inferred from the conventional charts. For instance the precise structure of the feature to the West of Scotland or the strong temperature gradients between the Irish Sea and the sea areas between Cornwall and south eastern Ireland. A warmer (greater than 7 K) patch of water on the Dogger Bank is also evident in the satellite data. One or two of the features however may still be artefacts caused by incomplete cloud clearing such as the plume of warm water reaching into the North Sea from the Dutch-German border. Figure 4 shows the day/night temperature difference image for the seven days of data. In general the SST differences are close to zero but near to the coasts the daytime values were up to 4 K warmer than the corresponding nighttime values which would be expected over shallow coastal waters. The absence of large positive temperature differences over the open sea is evidence that a diurnal thermocline was not present during these seven days. The small number of negative differences (i.e. where the nighttime SST is greater than the daytime values) is probably due to inadequate cloud clearing.

The absolute satellite SST values are in qualitative agreement with the conventional charts. A more comprehensive comparison of satellite SSTs computed using equation 1 and the ship SSTs was carried out by Llewellyn-Jones et al. (1984) showing the root mean square difference between the two was 0.53 K with a bias of -0.10 K. The satellite measures a surface skin temperature so the two measurements will only agree if the skin temperature is representative of the underlying bulk water temperature. There are two effects which can produce a significant difference between the bulk water temperature and the skin temperature. The first is the 'skin effect' which causes the skin temperature to be normally a few

tenths of a degree colder than the bulk temperature as observed by Robinson et al. (1984). The second effect is caused by the formation of a diurnal thermocline, which occurs when the top layers of the ocean are not well mixed when there are low surface wind speeds. Under these conditions the incident solar radiation can heat up the uppermost layers (usually a few tens of centimetres thick) of sea surface. This results in a surface skin temperature up to a few degrees warmer than the bulk water temperature during the early afternoon which is the time of the NOAA 9 daytime overpass. The evidence of figure 4 shows that this effect was not significant for the data presented here.

5. CONCLUSIONS

A sea surface temperature image was produced from fourteen passes of NOAA 9 data during the period 14-20 April 1985. However, even over this seven day period some pixels in the output image were cloud contaminated for every pass. More NOAA 9 passes per day could be processed rather than the two used here which would improve the coverage a little. When the second NOAA polar orbiter satellite is operational then data from this satellite will help reduce the number of cloud contaminated areas. Compared with conventional charts the satellite product gives good agreement in absolute SST values but also shows far more detail than can be inferred from the conventional charts. It is questionable whether most forecasting applications need such a high resolution product but for checking the conventional chart by filling in data void areas where there are no ship reports this product would undoubtedly be useful. In addition this new satellite product would be useful for such applications as deriving a local high-resolution SST climatology and location of ocean fronts (fisheries and other applications). It is also possible to obtain high resolution land surface temperatures from these data. However the interpretation of composite products is complicated - different areas contribute to the composite on different days, and the product is biased because it applies only to cloud free cases. Nevertheless, surface temperature is just one example of a product which may be derived from AVHRR data; high resolution climatologies of cloud cover, snow cover, surface albedo and other parameters could also be generated using a similar approach.

6. REFERENCES

- Eyre, J.R., Brownscombe, J.L. and Allam, R.J. 1984 Detection of fog at night using Advanced Very High Resolution Radiometer (AVHRR) imagery. *Met Mag*, 113, 266-271
- Lauritson, L., Nelson, G.J. and Porto, F.W. 1979 Data extraction and calibration of TIROS-N/NOAA radiometers. NOAA Tech. Memo. NESS 107
- Llewellyn-Jones, D.T., Minnett, P.J. Saunders, R.W. and Zavody, A.M. 1984 Satellite multichannel infra-red measurements of sea surface temperature of the N.E. Atlantic Ocean using AVHRR/2. *Quart. J. Roy. Met. Soc.*, 110, 613-631
- Mork, M. 1981 Circulation phenomena and frontal dynamics of the Norwegian coastal current. *Phil. Trans. R. Soc. London*, A.302, 635-647
- Robinson, I.S., Wells, N. and Charnock, H. 1984 The sea surface thermal boundary layer and its relevance to the measurement of sea surface temperature by airborne and spaceborne radiometers. *Int. J. Remote Sensing*, 5, 19-46
- Saunders, R.W., Ward, N.R., England, C.F. and Hunt, G.E. 1982 Satellite observations of sea surface temperature around the British Isles. *Bull. Amer. Meteor. Soc.*, 63, 267-272
- Saunders R.W. 1986 An automated scheme for the removal of cloud contamination from AVHRR radiances over Western Europe. *Int. J. Remote Sensing*, 7 (in press)
- Schwalb A. 1978 The TIROS-N/NOAA A-G satellite series. NOAA Tech. Memo. NESS 95.

Table 1Data from 14 NOAA 9 passes used in this study.

Date	Time GMT over dundee	Node
14/4/85	0351	Southbound
	1345	Northbound
15/4/85	0340	Southbound
	1335	Northbound
16/4/85	0330	Southbound
	1324	Northbound
17/4/85	0319	Southbound
	1313	Northbound
18/4/85	0308	Southbound
	1303	Northbound
19/4/85	0257	Southbound
	1252	Northbound
20/4/85	0247	Southbound
	1422	Northbound

Figure 1

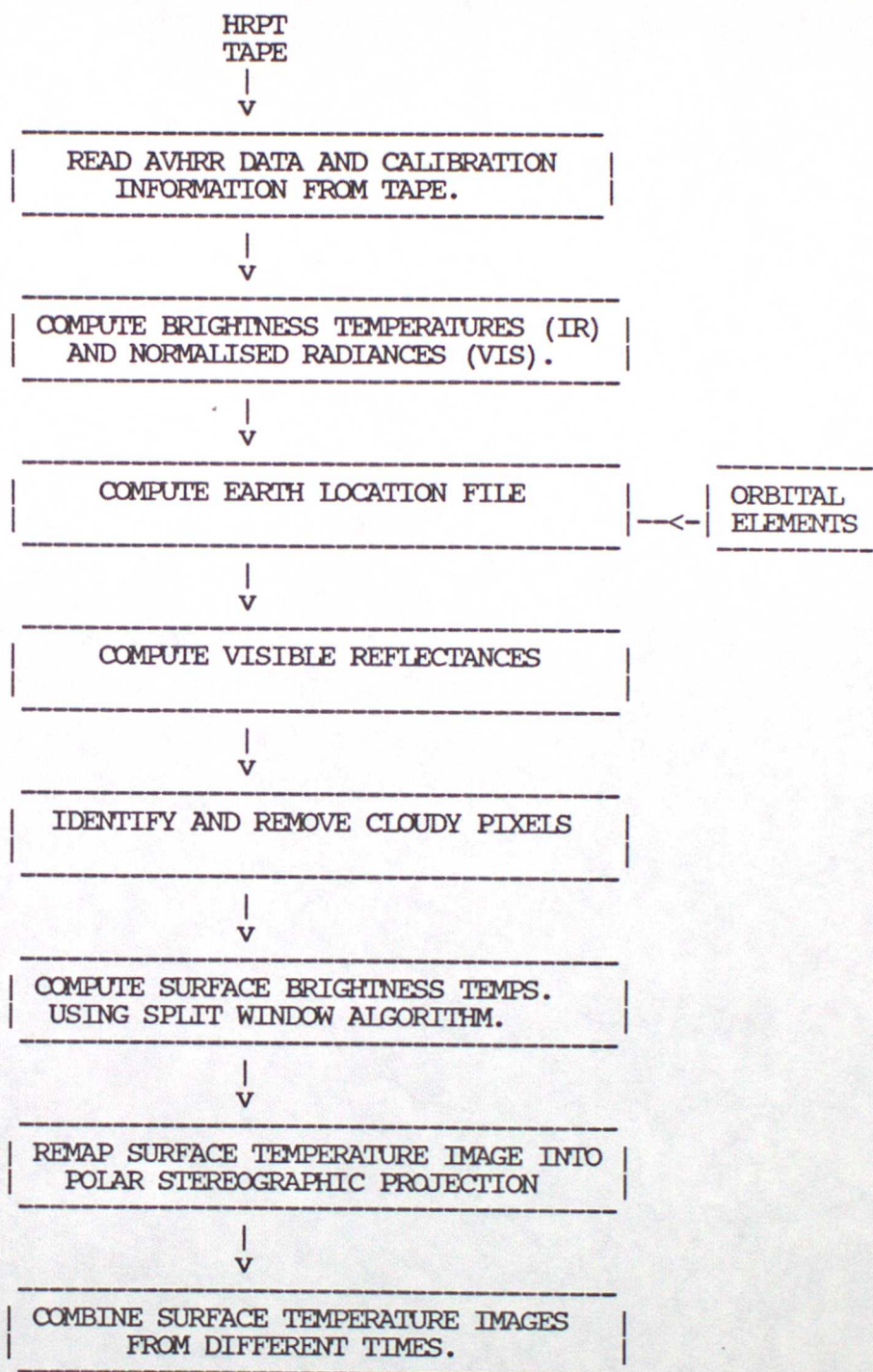


Figure 1 Flow diagram of overall AVHRR processing scheme for production of sea surface temperature images.

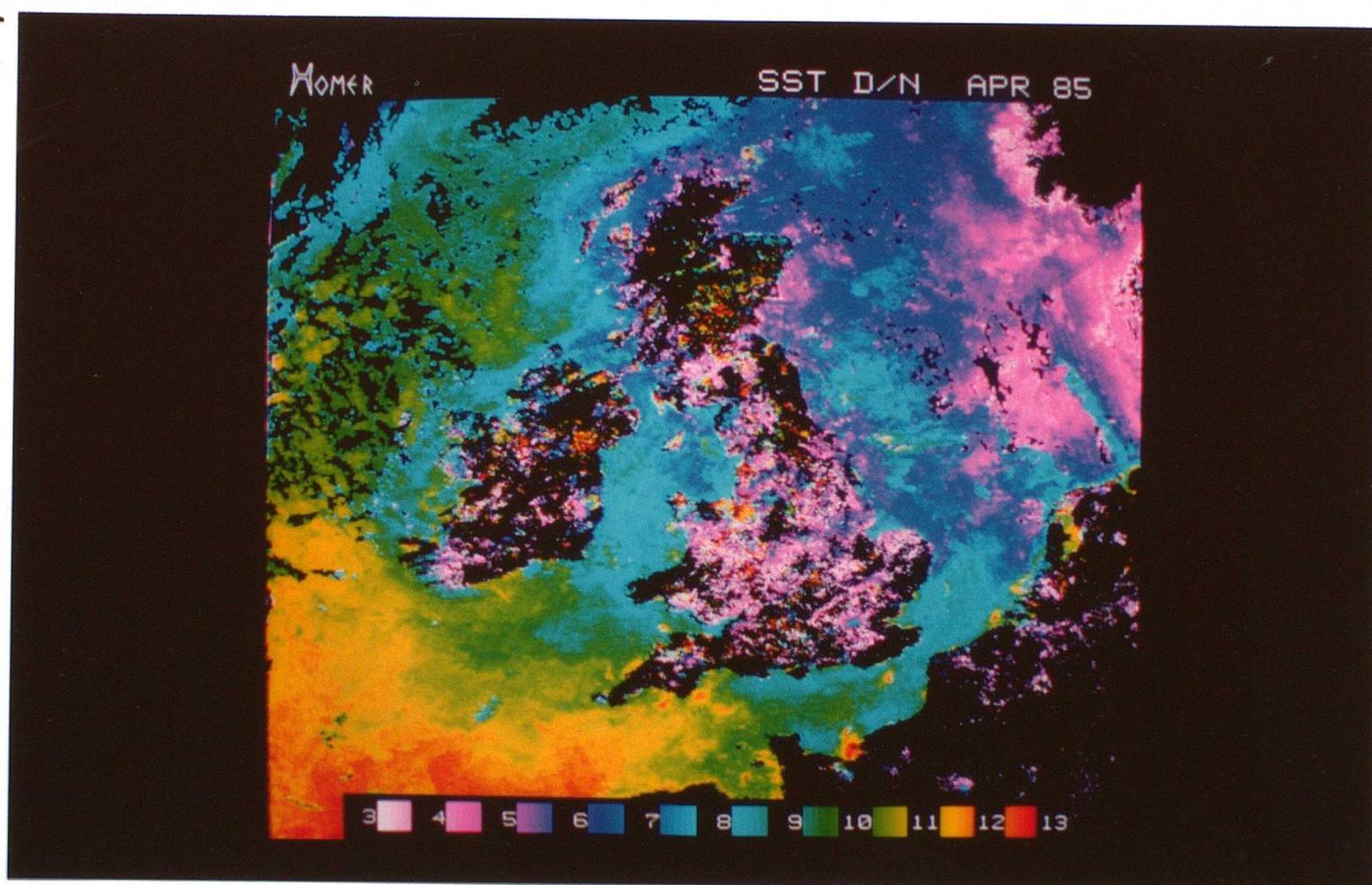


Figure 2 A composite image which combines cloudfree AVHRR data from seven daytime and nighttime passes for 14-20 April 1985. Over the sea black areas remained cloud covered during all fourteen passes. Over the land the temperatures were mostly outside the range of the colour table and hence also appear black. The scale at the bottom shows temperatures in K.

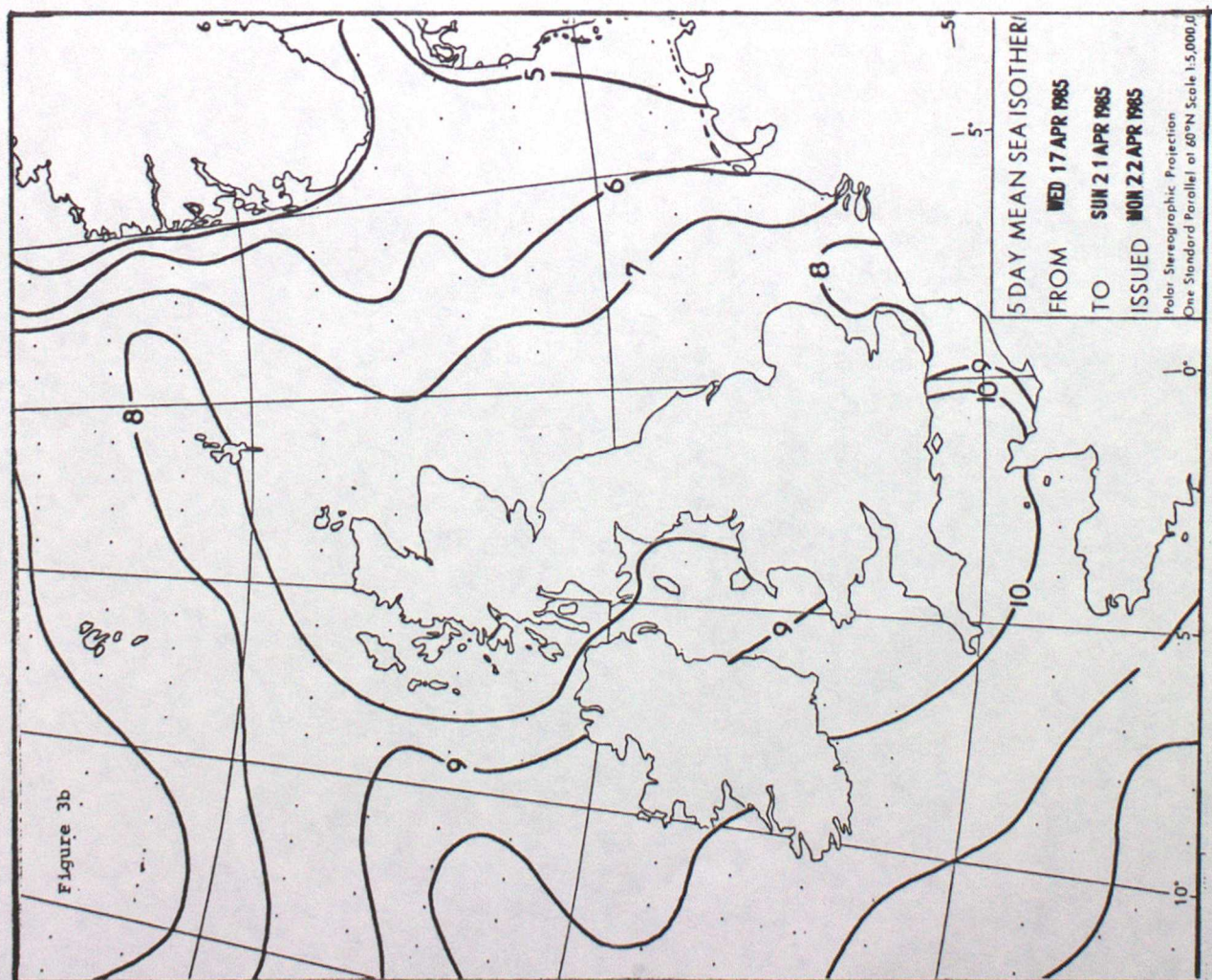
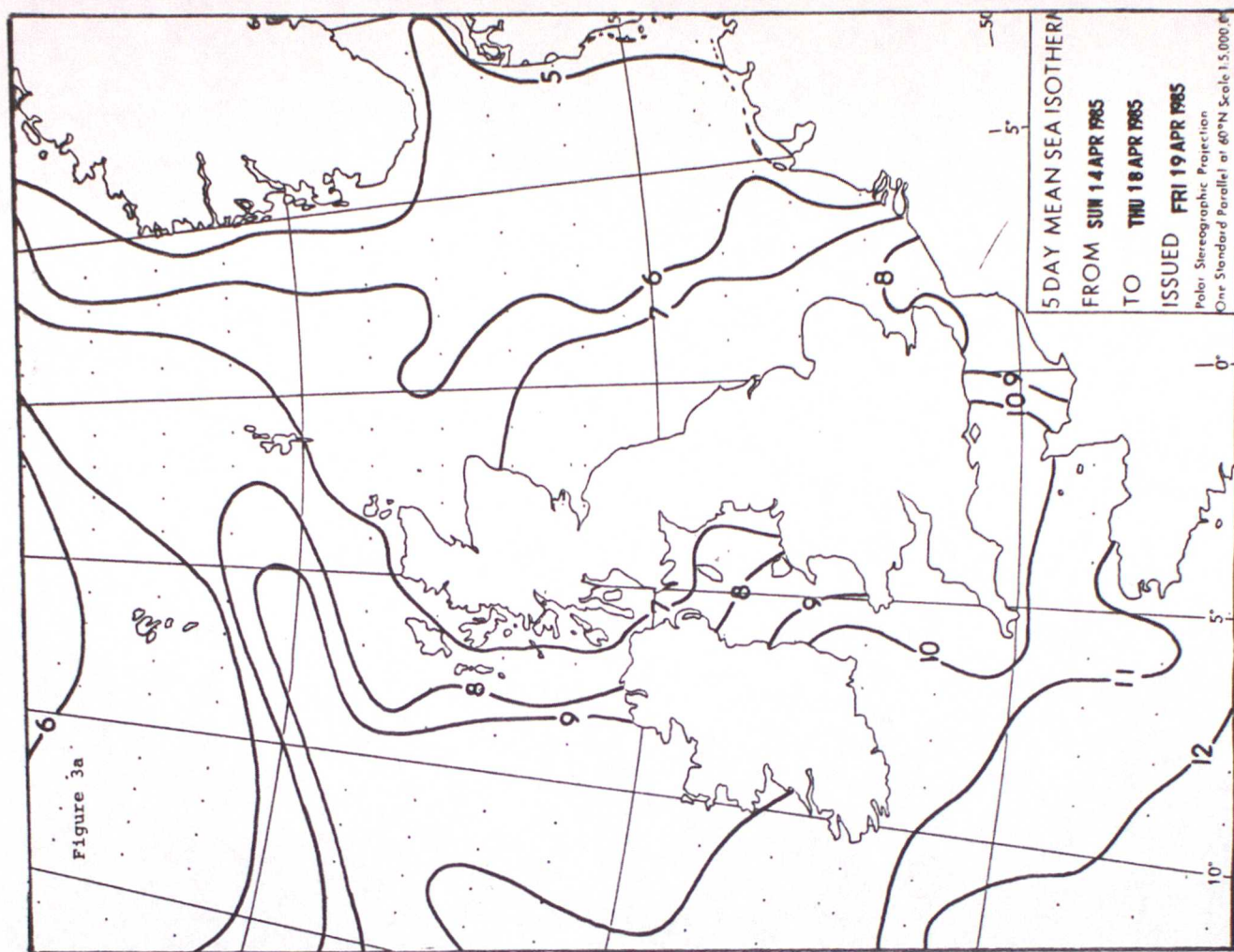


Figure 3 Conventional 5 day mean SST contour charts for the seas around the British Isles for (a) 14-18 April and (b) 17-21 April 1985.

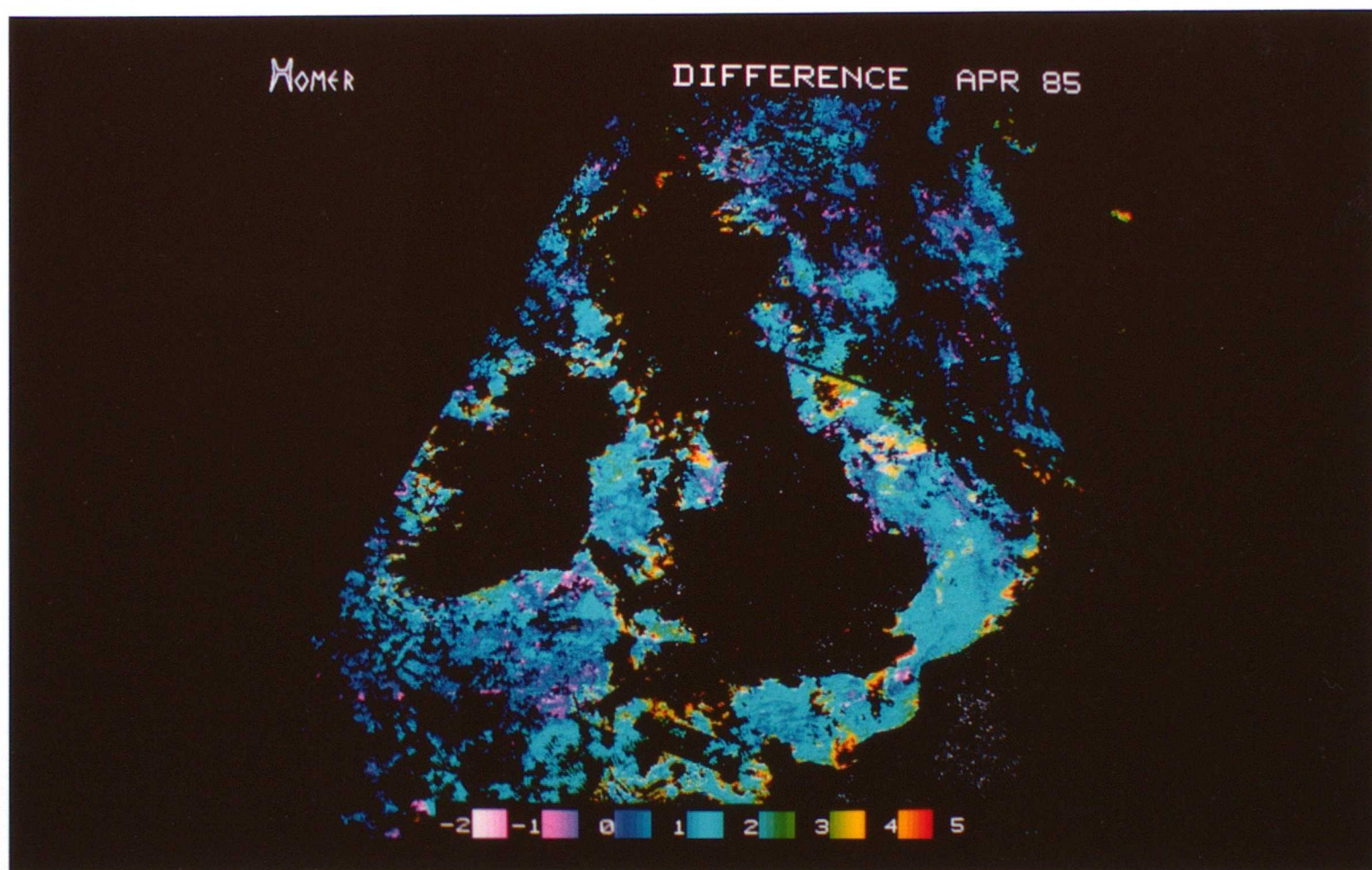


Figure 4 A day-night temperature difference image computed from AVHRR data for the period 14-20 April 1985. The scale at the bottom shows temperatures differences in K.

APPENDIX A

PROGRAMMING ASPECTS.

Programs on HERMES/HOMER used for processing AVHRR data are described below.

Some passes from Dundee require more than one Computer Compatible magnetic Tape CCT with the split in the data often occurring over the British Isles. In these cases the required channel data are extracted from each (CCT) independently and then the northern and southern portions of the pass are joined using program AVHRR/JOIN. The calibration file is likewise joined using AVHRR/JOINCAL. JOINCAL should be run first as it computes the number of lines overlap between the two images. The nighttime scheme currently rotates the images through 180 degrees so that the images appear with north at the top on the display device. This is not necessary in an operational scheme as the "rotating" could be done at the reprojection stage.

Figures A1 and A2 show the programming flow charts for processing the data on the Met O 19 VAX 11/750 computers. All programs (except AVHIN, PSIMAGE, PSIMOD, COLIM) are invoked by the AVHRR/... command where the particular processing option as indicated in figure A1 is supplied after the /. Help files exist on the system to explain the operation of these programs in more detail. Users are advised to compile a DCL command file to carry out the non-interactive parts of the processing scheme if they intend producing SST images on a regular basis.

It took 5 minutes of CPU time on a VAX 11/750 to reproject a 1024 x 1024 pixel image into a polar stereographic projection.

The timings for running the median filter program on a 1024 by 1024 image, on the HOMER VAX 11/750 with floating point accelerator were as follows : -

BOX SIZE	CPU TIME (approx.)
3	18 Min.
5	52 Min.
7	1Hr. 52 Min.
9	3Hr. 5 Min.

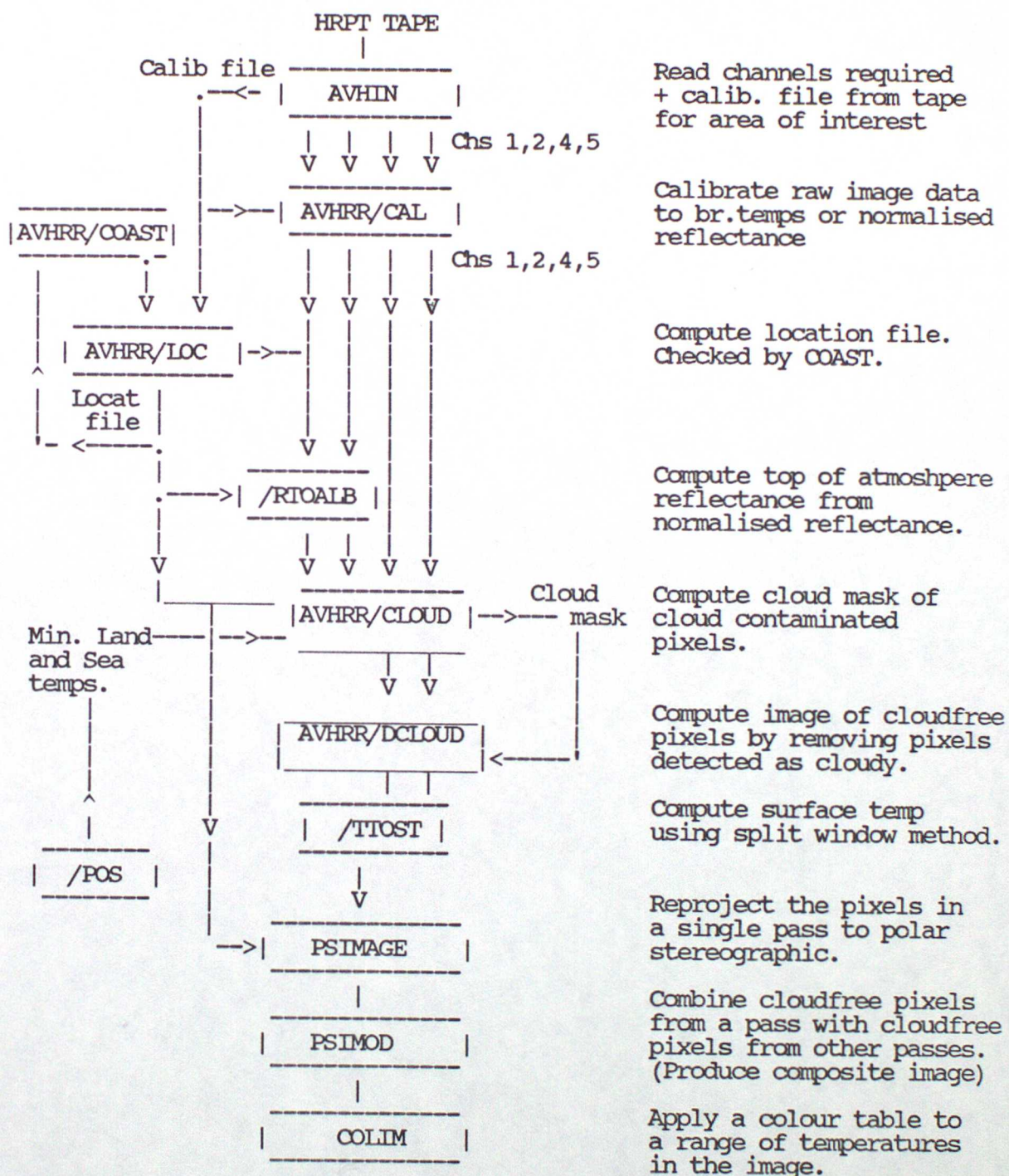
IMAGE ENHANCEMENT - COLOUR TABLE.

In these sea surface temperature images, the pixel counts have been scaled to an appropriate range of temperatures. A colour look up table is applied to the data for a selected range of temperatures to bring out the contrast of particular features (e.g. overall SST, localised SST features, etc). Seven colours are used representing

colder to warmer temperatures. They are white, violet, blue, cyan, green, yellow, red. The selected range of temperatures are then scaled to use the full range of colours. White corresponding to the coldest temperatures, red corresponding to the highest. A ramped or stepped transition of colours across the chosen range can be selected. A scale showing which colour corresponds to which range of temperatures is displayed along the bottom of the image.

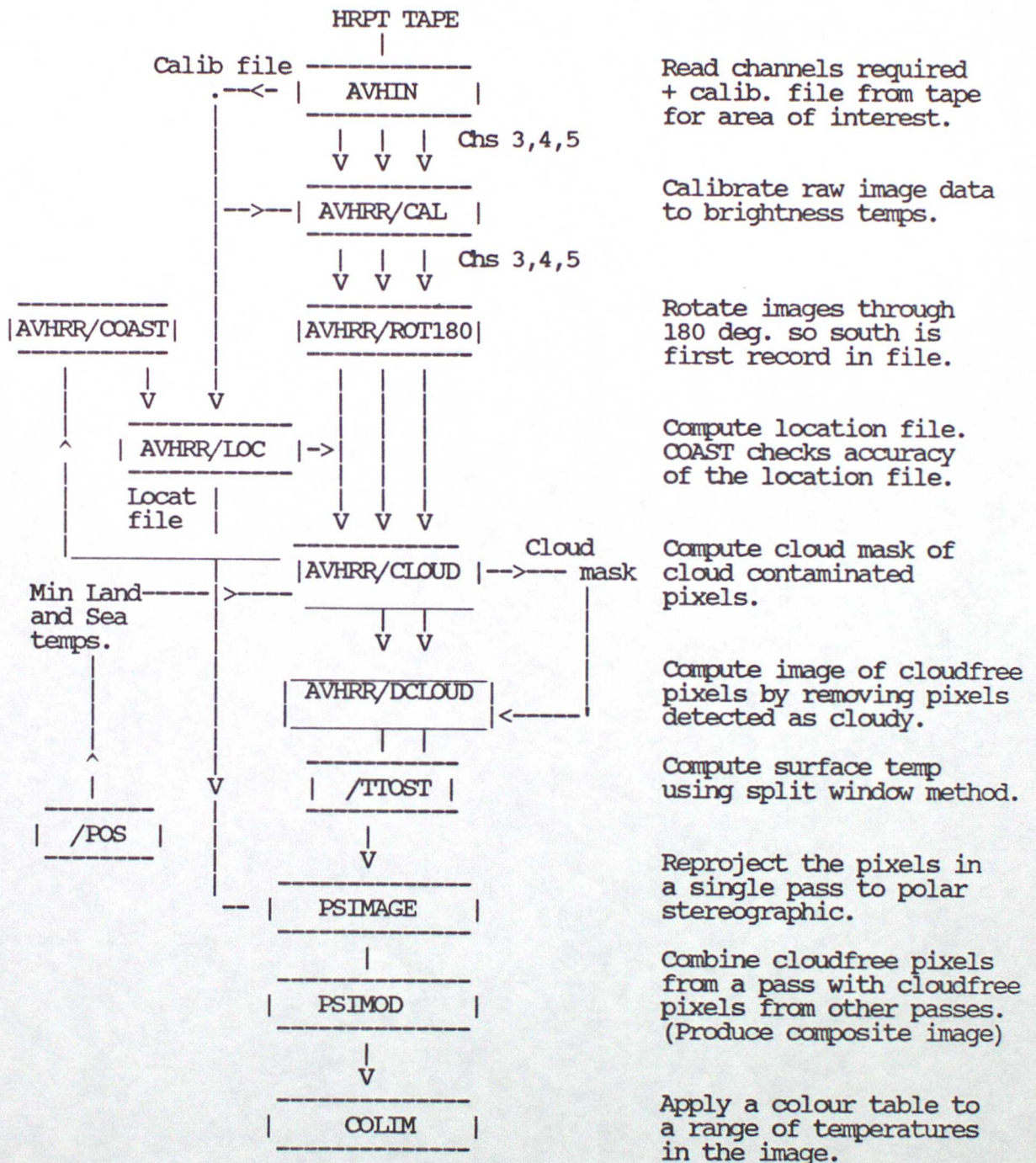
Finally a coastline and/or latitude/longitude grid, can be overlaid on to the polar stereographic image if desired.

FIGURE A1
DAYTIME PROCESSING FLOWCHART



Colour Composite polar stereographic
high resolution sea surface temperature image.

FIGURE A2
NIGHTTIME PROCESSING FLOWCHART

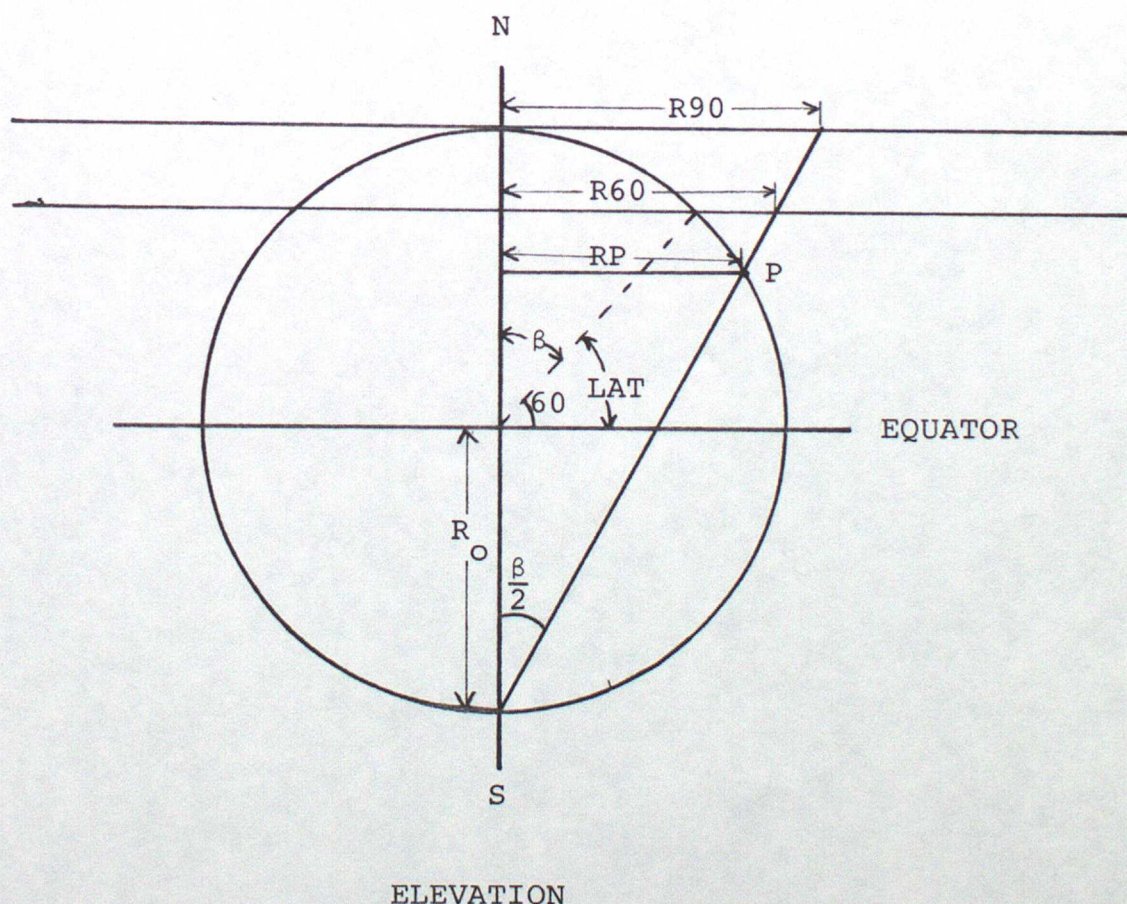


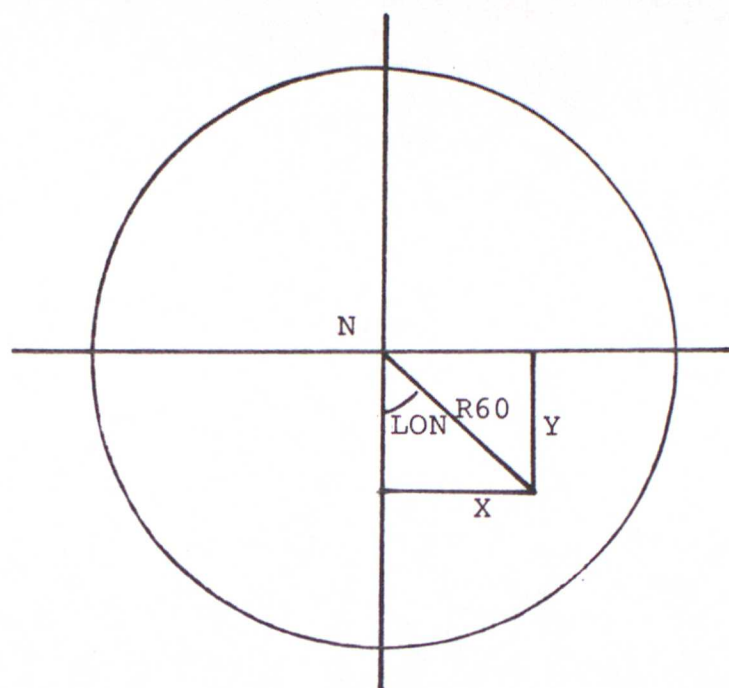
Colour Composite polar stereographic
high resolution sea surface temperature image.

APPENDIX B

POLAR STEREOGRAPHIC PROJECTION ON THE ARGS.

This essentially simple process remaps the SST image as viewed by the satellite onto a polar stereographic projection plane at 60 degrees latitude. A scale of 1.5 km/pixel was chosen. At this scale sometimes more than one pixel from the input is mapped to a pixel in the output polar stereographic image. Because of the large number of data points in an image not every pixel is earth located. It was found that if latitudes and longitudes are held on a 32 x 32 grid, this is an acceptable compromise between accuracy and data storage requirements. Also to save on memory storage requirements 32 AVHRR lines are reprojected at a time. If only part of an image is to be reprojected (e.g. Scotland), a new location file had to be recreated by interpolation from the original location file. First the corners of the 32 x 32 pixel array which are earth located are mapped to X, Y coordinates in the polar stereographic projection. Then pixels within the 32 x 32 box are earth located using linear interpolation by subroutine INTP.





PLAN

$$R60 = 2 \times R0 \times \tan [(90 - \text{LAT})/2] \times \text{SCA} \quad \text{-----} \quad (1)$$

$$\text{and} \quad \begin{aligned} X &= R60 \times \sin [\text{LON}] \\ Y &= R60 \times \cos [\text{LON}] \end{aligned} \quad \begin{array}{l} \text{-----} \quad (2) \\ \text{-----} \quad (3) \end{array}$$

$$\text{where} \quad \text{SCA} = 1.5 \times \cos(15) \times \cos(15) \quad \text{-----} \quad (4)$$

- RP is the perpendicular distance from the earth's axis to the point P on the circumference of the earth.
- R90 is the distance from the pole to the reprojection of point P on a 90 degree latitude polar stereographic projection plane.
- R60 is the perpendicular distance from the earth's axis to the reprojection of point P on a 90 degree latitude polar stereographic projection plane.
- R0 is the radius of the earth (6371.0 km.).
- LAT is the latitude of point P in degrees.
- LON is the longitude of point P in degrees.
- X is the X coordinate of the point on the ARGS screen.
- Y is the Y coordinate of the point on the ARGS screen.
- SCA is used to scale of the output image for reprojection onto the ARGS, this includes a factor for reproject onto the 60 degree latitude plane.
The reprojection factor used is 1.5 km/pixel.

This projection is performed by subroutine PSLIXY.